

## Research Article

# Synergistic Effects of Fractional CO<sub>2</sub> Laser and Recombinant Humanized Type III Collagen (rhCol III) in Atrophic Acne Scar Treatment: Activation of MAPK Pathway and Enhanced Collagen Remodeling

Li Gu <sup>1</sup>, Jing Wang,<sup>1,2</sup> Rong Guo,<sup>3</sup> Zhinan Shi,<sup>4</sup> Zhiyi Xu,<sup>1,2</sup> Shu Zhou,<sup>1</sup> Jingting Zhao,<sup>1</sup> Liqun Gu,<sup>1</sup> Bingrong Zhou <sup>5</sup> and Hui Hua <sup>1</sup>

<sup>1</sup>Department of Dermatology, Nantong Third People's Hospital, Affiliated Nantong Hospital 3 of Nantong University, Nantong, China

<sup>2</sup>Medical School of Nantong University, Nantong, China

<sup>3</sup>Department of Dermatology, Shanxi Bethune Hospital, Taiyuan, China

<sup>4</sup>Department of Dermatology, Ren Ji Hospital, Shanghai Jiaotong University School of Medicine, Shanghai, China

<sup>5</sup>Department of Dermatology, The First Affiliated Hospital of Nanjing Medical University, Nanjing, China

Correspondence should be addressed to Bingrong Zhou; zhoubingrong@njmu.edu.cn and Hui Hua; huahui@ntu.edu.cn

Received 17 March 2025; Revised 7 September 2025; Accepted 28 October 2025

Academic Editor: Suraiya Saleem

Copyright © 2025 Li Gu et al. Dermatologic Therapy published by John Wiley & Sons Ltd. This is an open access article under the terms of the Creative Commons Attribution License, which permits use, distribution and reproduction in any medium, provided the original work is properly cited.

**Background:** Fractional CO<sub>2</sub> laser (FCL) is widely used for resurfacing the skin with atrophic acne scars. This study aims to explore the synergistic efficacy of recombinant humanized type III collagen (rhCol III) on FCL in treating atrophic acne scars. **Methods:** A total of 20 patients with facial atrophic acne scars from two medical institutions were treated with a single session of full-face FCL. One month post-FCL, they were randomly assigned to the FCL + rhCol III group and FCL + NC group, with 10 cases per group. Patients in the FCL + rhCol III group received dermal injections with 4 mg of rhCol III dissolved in 1.2 mL of saline on one side of the face, and those in the FCL + NC group were similarly injected with the same amount of saline. Dermal injections were performed three times, with an interval of 4 weeks. Therapeutic efficacy was assessed using the Echelle d'évaluation clinique des cicatrices d'acné (ECCA) grading scale and the Global Scarring Grading System (GSS). Human dermal fibroblasts (HDFs) were cultured in vitro, and induced with FCL and rhCol III. Immunofluorescence was utilized to detect the expression of type I and III collagens. RNA-sequencing (RNA-seq) identified differentially expressed genes (DEGs) in HDFs induced with FCL combined with rhCol III.

**Results:** A total of 18 eligible patients were enrolled and followed up. Post-treatment, patients in the FCL + rhCol III group were graded with a significantly lower ECCA score ( $77.50 \pm 15.07$  vs.  $106.1 \pm 21.25$ ,  $p < 0.05$ ), but a higher scar improvement rate ( $40.23\% \pm 13.23\%$  vs.  $23.26\% \pm 19.69\%$ ,  $p < 0.05$ ) than those in the FCL + NC group. Classified by the type of acne scars, patients with boxcar and icepick acne scars significantly benefited more from FCL combined with rhCol III than those in the FCL + NC group and showed a significantly reduced ECCA score and an increased scar improvement rate ( $p < 0.05$ ). Similarly, patients in the FCL + rhCol III group also exhibited significantly a lower GSS score ( $7.75 \pm 1.75$  vs.  $10.00 \pm 2.33$ ,  $p < 0.05$ ) and a higher scar improvement rate ( $43.30\% \pm 10.49\%$  vs.  $25.59\% \pm 18.34\%$ ,  $p < 0.05$ ). In vitro experiments showed that the induction of FCL combined with rhCol III significantly upregulated type I and III collagens in HDFs. RNA-seq unmasked that MAPK signaling pathway was activated in HDFs induced with FCL combined with rhCol III.

**Conclusion:** FCL combined with rhCol III effectively reduces facial atrophic acne scars through the activation of the MAPK pathway.

**Keywords:** atrophic acne scars; FCL; MAPK signaling pathway; rhCol III; RNA-seq

## 1. Introduction

Acne vulgaris is a chronic inflammatory skin disease that affects hair follicles and sebaceous glands [1]. Approximately 80% of adolescents may develop acne vulgaris, and up to 43% of them experience varying degrees of scarring [1, 2]. Acne scars can be hypertrophic or atrophic, with the latter being more common [3]. Atrophic acne scars can be further categorized into three subtypes: boxcar, rolling, and icepick varieties [4]. Acne scarring not only impairs facial aesthetics but also induces psychological issues such as anxiety, low self-esteem, depression, and social disorders [5, 6]. More effective treatments are needed to address these issues.

Current treatments for atrophic acne scars include surgical excision, dermal fillers, chemical peels, fractional microneedle radiofrequency, and fractional CO<sub>2</sub> laser (FCL) [7, 8]. FCL delivers energy that is absorbed by the water in the skin, creating fractional thermal damage that penetrates into the dermis. This effect promotes the contraction, regeneration, and remodeling of collagen, resulting in the generation of new, well-arranged collagen fibers [9]. Four sessions of FCL greatly decrease the depth of atrophic scars by an average of 42%, and the Patient and Observer Scar Assessment Scale (POSAS) score by 32.7% [10]. Our previous study demonstrated an excellent performance of the ultra-pulse CO<sub>2</sub> laser combined with FCL in reducing atrophic acne scars, with a reduction of the Echelle d'évaluation clinique des cicatrices d'acné (ECCA) score from 162.7 to 93.1 [11]. However, monotherapy with FCL may result in clinical complications, including erythema, edema, and postinflammatory hyperpigmentation [9]. Thus, various combinations have emerged as a new trend in treating atrophic acne scars.

Recombinant humanized type III collagen (rhCol III), engineered from the sequence of human collagen type III, is tailored for tissue repair and wound healing [12, 13]. Due to its superior solubility and cell adhesion properties, rhCol III has been extensively utilized in alleviating skin photoaging. The rhCol III hydrogel, when combined with microneedle technology, potently heals infectious chronic diabetic wounds by inhibiting inflammatory responses, promoting cell proliferation, and angiogenesis [13]. Wang et al. revealed that rhCol III mitigates UV-induced skin photoaging by stimulating the expression of the extracellular matrix (ECM) [14]. In mice with myocardial infarction during the late proliferative phase, rhCol III significantly restores the mechanical properties of the myocardium and reduces scar size [15].

In the present study, we examined the efficacy of FCL combined with rhCol III in treating atrophic acne scars and uncovered the underlying molecular mechanisms. Our findings provided evidence supporting the broader clinical application of FCL combined with rhCol III. To achieve this, we conducted a series of experiments, including cell culture, Cell Counting Kit-8 (CCK-8) assay, immunofluorescence, and RNA-sequencing (RNA-seq), to investigate the effects of FCL combined with rhCol III on atrophic acne scars. By analyzing the data obtained from these experiments, we aimed to elucidate the molecular mechanisms underlying

the efficacy of this combined treatment. The results of our study not only enhance our understanding of the pathogenesis of atrophic acne scars but also pave the way for potential therapeutic strategies to improve the quality of life for patients suffering from this condition.

## 2. Materials and Methods

**2.1. Participants.** From October 2022 to October 2023, 20 patients with facial atrophic acne scars and the Fitzpatrick skin type II–IV were enrolled, including 10 from Nanjing Yijia Medical Aesthetic Clinic and the remaining 10 from Taiyuan Vitiligo Hospital. After excluding two patients without complete clinical data, a total of 18 eligible ones were finally included. The sample size was estimated a priori using G\*Power (version 3.1.9.7). Based on prior data [11], we assumed a mean difference in ECCA scores of 28.6 points and a common standard deviation (SD) of 18.5 points between groups. With 80% statistical power and a two-sided  $\alpha$  level of 0.05 (independent *t*-test), a minimum of seven participants per group was required. To account for a potential 20% dropout rate, we planned to recruit nine participants per group, resulting in a total target sample size of 18. This study was approved by the Ethics Committee of Nanjing Yijia Medical Aesthetic Clinic (Ethics Number: 2022-10-10) and the Taiyuan Vitiligo Hospital (Ethics Number: 2022001). Excluded were those with allergies to lidocaine or rhCol III; incomplete clinical data; previous or ongoing laser, radiofrequency, or surgical treatments within 3 months prior; pregnancy or breastfeeding. The study flowchart is shown in Figure 1.

### 2.2. Treatment Procedures

**2.2.1. Preoperative Preparation.** Facial condition assessment and facial skin cleansing were conducted prior to FCL. The VISIA skin analysis system (Jiangsu Beining Intelligent Technology Development Co., Ltd., China) captured left, right, and frontal facial images before and after the treatment. The lasered area was topically applied with a compound lidocaine cream (Tsinghua Ziguang Co., Ltd., Beijing, China) and covered with a plastic wrap for 1 h prior to iodophor disinfection.

**2.2.2. Intraoperative Treatment.** A full-face FCL was performed on bilateral sides of the face. Briefly, patients in the Nanjing Yijia Medical Aesthetic Clinic were treated with the Alma Femilift ultra-pulse FCL (Femilift, Alma™ Lasers, Caesarea, Israel) with the Pixel handpiece in an aesthetic mode at a density of  $7 \times 7$  and an energy of 20–40 mJ/pixel. Patients in the Taiyuan Vitiligo Hospital were treated with the Lumenis ultra-pulse FCL (Lumenis Inc., Santa Clara, CA, USA) in a fractional mode in the following settings: the DeepFX setting (spot 1–5, spot size 1–10 mm, energy 12.5–30 mJ, density 5%, frequency 100–250 Hz, repeated delay 1 s); the ActiveFX setting (spot 1–7, spot size 1–9 mm, energy 125–225 mJ, frequency 100–250 Hz, density 5%); and DeepFX combined with ActiveFX mode. Treatment

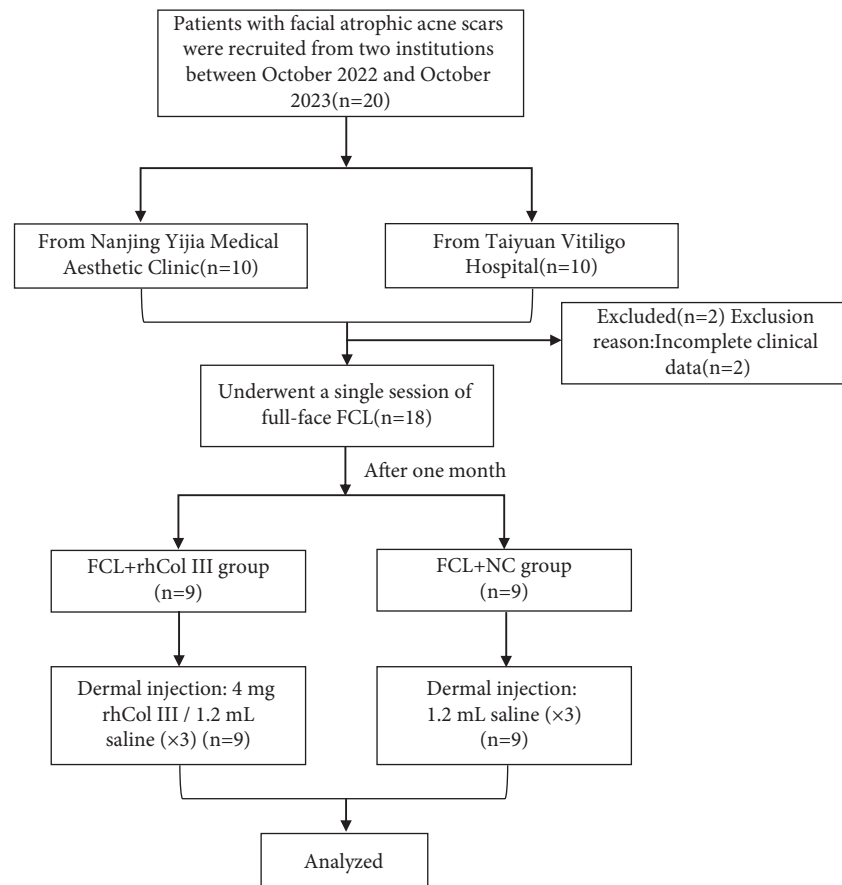


FIGURE 1: The flowchart of participant enrollment, allocation, and follow-up.

parameters were adjusted based on individual age, Fitzpatrick skin type, location and extent of acne scars, and skin texture. All patients were treated with one session of FCL.

**2.2.3. Postoperative Treatment.** At 1 month after FCL, patients were randomly assigned to the FCL + NC group and FCL + rhCol III group, with nine cases per group. Patients in the FCL + NC group were dermally injected with 1.2 mL of normal saline as controls, while those in the FCL + rhCol III group received dermal injections of 4 mg rhCol III (Shanxi Jinbo Biomedical Co., Ltd., 4 mg/vial) dissolved in 1.2 mL of saline. Briefly, the atrophic and depressed scar areas were marked. Three dermal injections were performed into the base of the scar within the marked area using 1 mL syringes with caps, with an interval of 4 weeks. Following each injection, the facial condition was assessed in a single-blind way.

**2.3. Efficacy Evaluation.** Facial images captured at baseline and during follow-up visits were used to evaluate the changes in acne scars. Atrophic acne scars were categorized by shape and size into icepick (V-shaped), boxcar (U-shaped), and rolling (M-shaped) scars. The ECCA grading scale and the Global Scarring Grading System (GSS) were adopted to evaluate the efficacy of FCL combined with rhCol III in treating acne scars. The scar improvement rate was calculated as follows: scar improvement rate (%) = (pretreatment ECCA/

GSS score-post-treatment ECCA/GSS score)/pretreatment ECCA/GSS score  $\times 100\%$ .

**2.4. Cell Culture and Treatment.** Approved by the Medical Ethics Committee of Nantong Third People's Hospital (No: EL2022007), human dermal fibroblasts (HDFs) were obtained from the foreskin of healthy male patients in the Department of Urology, Nantong Third People's Hospital and cultured in vitro as previously reported [16]. HDFs incubated in DMEM (Gibco, Thermo Fisher Scientific) were placed in an incubator at 37°C with 5% CO<sub>2</sub>. Those passaged in the generation 4–10 were used in *in vitro* experiments. HDFs were induced with blank control, FCL at an energy of 20 mJ and a density of 11.1% for 24 h, 1 mg/mL rhCol III for 24 h, or their combination.

**2.5. CCK-8 Assay.** Cell viability was assessed using an Enhanced CCK-8 (CCK-8, Beyotime Biotechnology, China). HDFs were implanted in 96-well plates and induced with 10  $\mu$ L of CCK-8 reagent per well for 2 h. The absorbance at 450 nm was measured using an enzyme-linked immunosorbent assay (ELISA) reader (Thermo Fisher Scientific, CA, USA).

**2.6. Immunofluorescence.** HDFs were cultured on glass coverslips, fixed with 4% paraformaldehyde (PFA) for 15 min, and permeabilized with 1% Triton X-100 for 15 min

at room temperature. After blocking nonspecific antibodies by immersing in 10% normal goat serum for 20 min, HDFs were incubated overnight at 4°C with the mouse anti-COL-I and anti-COL-III antibodies (1:500, Servicebio, China). On the following day, HDFs were incubated with the Alexa Fluor 488 and CY3 fluorescent secondary antibodies (1:400) at 37°C for 1 h in the dark and stained with 1 µg/mL DAPI (Sigma, USA) for 5 min at room temperature. Finally, HDFs were observed using a confocal microscope.

**2.7. RNA-Seq.** Total RNA was extracted from HDFs using TRIzol reagent (Takara, Shiga, Japan) and purified.

RNA integrity was evaluated using the Agilent 2100 Bioanalyzer. Library preparation, sequencing (conducted on the Illumina NovaSeq 6000 platform), quality control (performed with FastQC), and raw data generation were carried out by Shanghai Biochem Biotechnology Co., Ltd., a specialized genomics service provider. Subsequent bioinformatic analyses—including read alignment to the reference genome GRCh38 using HISAT2, gene expression quantification, and identification of differentially expressed genes (DEGs)—were performed collaboratively by Zhinan Shi from our research team and the bioinformatics team supervised by Professor Bingrong Zhou at the First Affiliated Hospital of Nanjing Medical University. DEGs with  $P_{adj} < 0.05$  and  $|\log \text{ fold change (FC)}| \geq 1$  were identified. Gene Ontology (GO) and Kyoto Encyclopedia of Genes and Genomes (KEGG) analyses were conducted using the DAVID database (<https://david.ncifcrf.gov/>), and the results were analyzed by the R package and visualized using Cytoscape software.

**2.8. Statistical Analysis.** Data expressed as mean  $\pm$  SD were analyzed using GraphPad Prism 8 (GraphPad Software Inc., San Diego, CA, USA). Statistical analyses were performed using *t*-tests or one-way analysis of variance (ANOVA), if appropriate.  $p < 0.05$  was considered statistically significant.

### 3. Results

**3.1. Clinical Efficacy of FCL Combined With rhCol III.** After the treatment, the ECCA scores of patients in the FCL + NC group decreased significantly from  $142.2 \pm 27.82$  to  $106.1 \pm 21.25$  at baseline, whereas the ECCA scores of patients in the FCL + rhCol III group decreased significantly from  $132.8 \pm 27.82$  to  $77.50 \pm 15.07$  at baseline ( $p < 0.05$ ) (Figure 2(a)). A significantly higher scar improvement rate was observed in the FCL + rhCol III group than in the FCL + NC group ( $40.23\% \pm 13.23\%$  vs.  $23.26\% \pm 19.69\%$ ,  $p < 0.05$ ) (Figure 2(a)). We also graded the ECCA scores of V-shaped, U-shaped, and M-shaped atrophic acne scars (Figure 2(b)–2(d)). For V-shaped and U-shaped scars, FCL combined with rhCol III significantly decreased the ECCA score and increased the scar improvement rate more than the monotherapy of FCL ( $p < 0.05$ ). Although FCL combined with rhCol III achieved a lower ECCA score in patients with M-shaped scars than that at baseline, the therapeutic outcome remained similar with controls at the last follow-up visit.

Similarly, the post-treatment GSS score in the FCL + NC group decreased from  $13.75 \pm 2.91$  to  $10.00 \pm 2.33$ , whereas those in the FCL + rhCol III group significantly decreased from  $14.13 \pm 2.36$  to  $7.75 \pm 1.75$  ( $P < 0.05$ ) (Figure 2(e)). The scar improvement rate, based on the GSS scores, was also significantly higher in the FCL + rhCol III group ( $43.30\% \pm 10.49\%$  vs.  $25.59\% \pm 18.34\%$ ,  $p < 0.05$ ) (Figure 2(e)). Intuitively visualized in facial images, FCL combined with rhCol III was superior to the monotherapy of FCL in reducing acne scars (Figure 2(f),2(g)).

**3.2. FCL Combined With rhCol III Promotes the Proliferation of HDFs In Vitro.** Induction with rhCol III at various concentrations (0.05, 0.1, 0.5, and 1 mg/mL) markedly elevated the proliferative capacity of HDFs, most prominently at 1 mg/mL (Figure 3(a)). At a density of 11.1%, a stimulation of either 10 mJ or 20 mJ energy significantly stimulated the proliferation of HDFs ( $p < 0.05$ ). However, the proliferation of HDFs was significantly suppressed by FCL at a density of 100%, and an energy of both 10 mJ or 20 mJ (Figure 3(b)). In comparison to the single induction of FCL (density 11.1%, energy 10 or 20 mJ), co-induction with FCL and rhCol III significantly boosted the proliferation of HDFs ( $p < 0.05$ ), especially in the combination group of 20 mJ FCL and 1 mg/mL rhCol III (Figure 3(c)).

**3.3. FCL Combined With rhCol III Upregulates Type I and III Collagens in HDFs In Vitro.** The immunofluorescence results revealed significantly higher positive expressions of type I and III collagens in HDFs induced with FCL combined with rhCol III, compared to those induced with FCL alone ( $p < 0.05$ , Figure 4(a),4(b)), suggesting that the combination of FCL and rhCol III greatly promoted the production of new collagens.

**3.4. DEGs and Their Biological Functions Involved in the Efficacy of FCL Combined With rhCol III.** The correlation heatmap and principal component analysis revealed the intragroup and intergroup consistency, respectively (Figure 5(a),5(c)). A total of 1607 DEGs were identified between rhCol III-induced HDFs and negative controls, involving 883 upregulated and 724 downregulated. Between the FCL + rhCol III group and FCL group, there were 1518 DEGs, of which 1089 were significantly upregulated and 429 were downregulated (Figure 5(b)). Clusters of DEGs were visualized in a heatmap (Figure 5(d)).

**3.5. The MAPK Signaling Pathway Underlies the Efficacy of FCL Combined With rhCol III in Treating Acne Scars.** DEGs between rhCol III-induced HDFs and negative controls were significantly enriched in the following biological processes: regulation of cell population proliferation, fibroblast proliferation, cell division, cell migration, and the apoptotic process (Figure 6(a)). KEGG pathway enrichment analysis further indicated that these DEGs were predominantly involved in the MAPK signaling pathway and cytokine-cytokine receptor interactions (Figure 6(b)). A



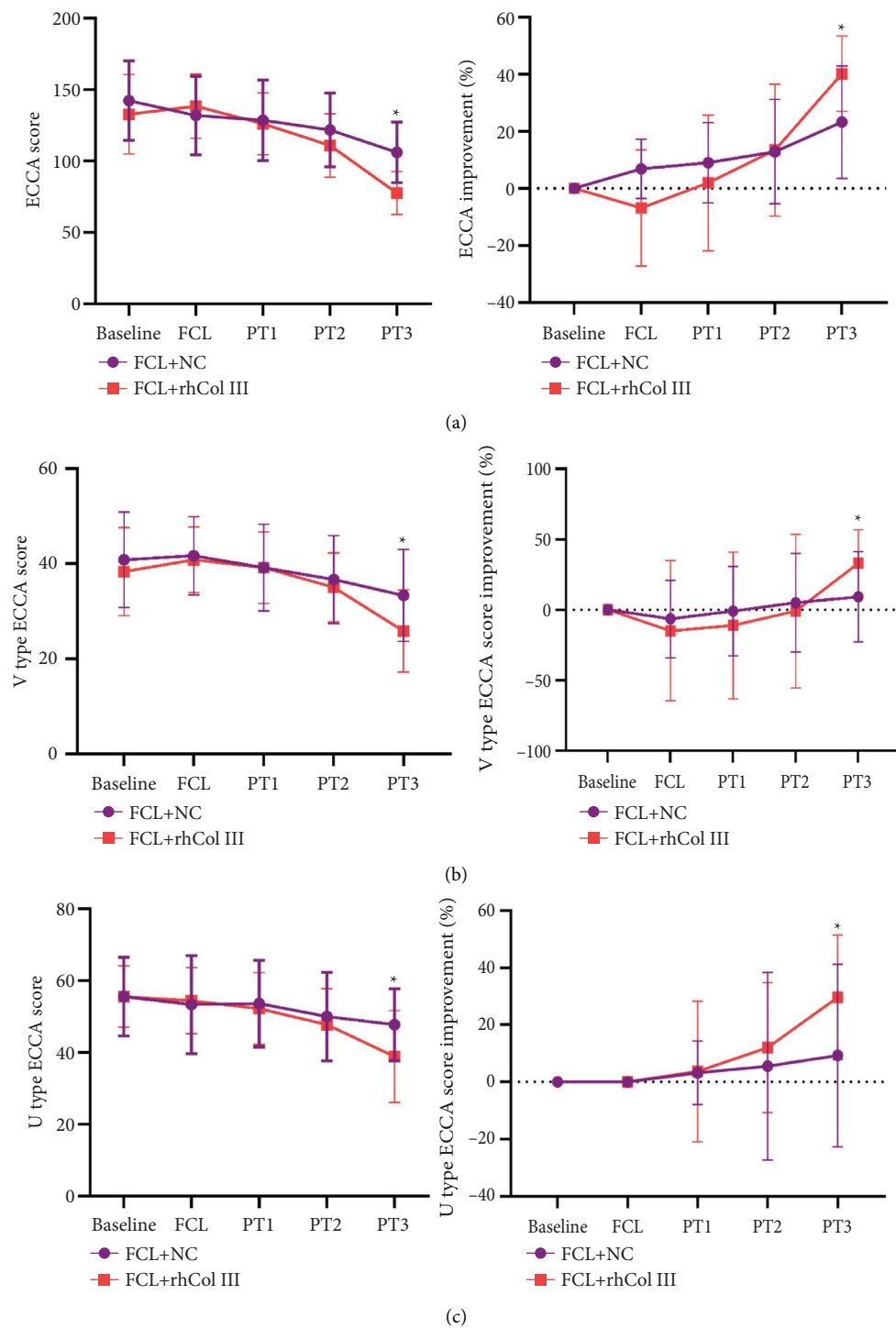


FIGURE 2: Continued.

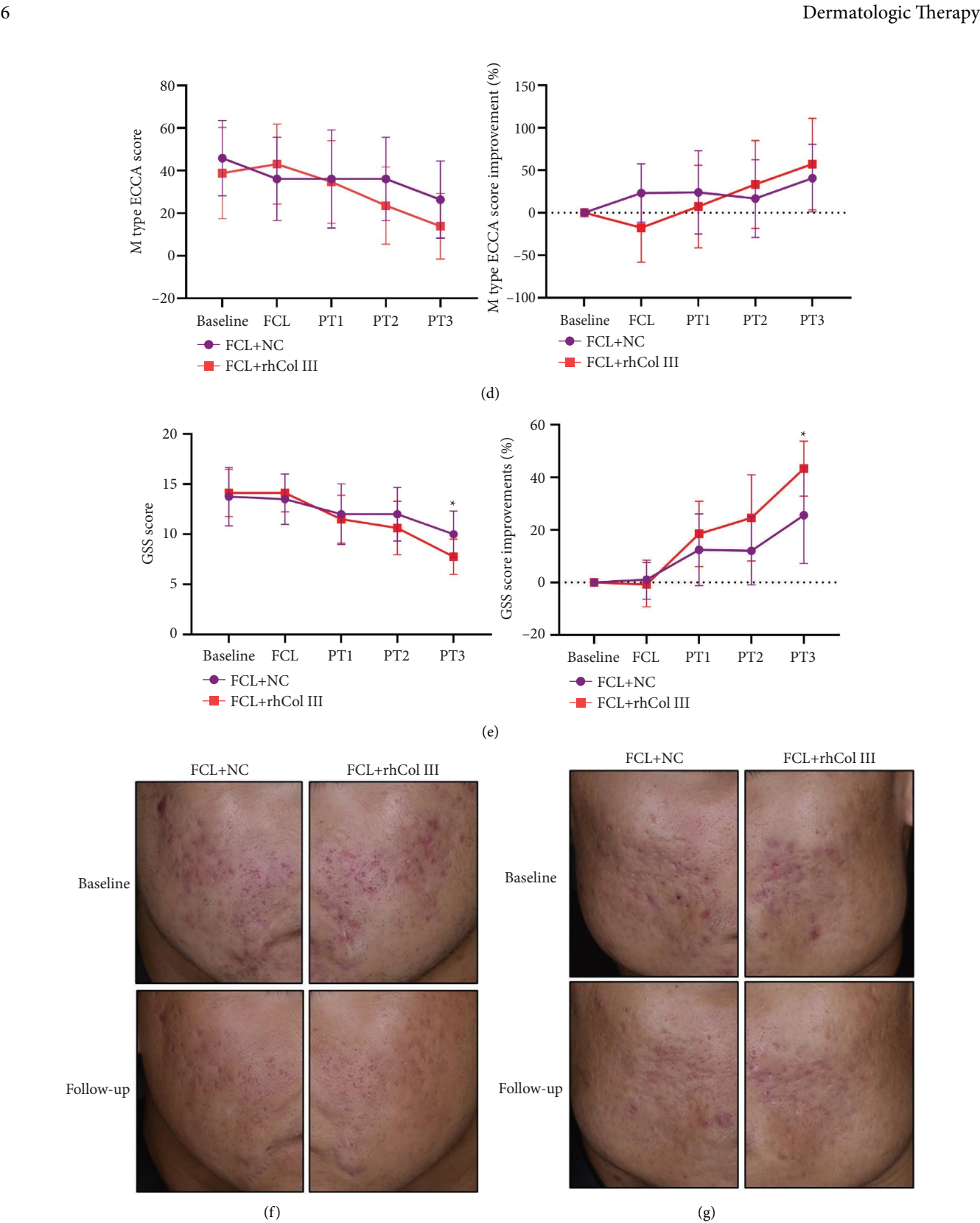


FIGURE 2: Clinical efficacy of FCL combined with rhCol III in treating atrophic acne scars. (a) The overall ECCA score and scar improvement rate. (b–d) The ECCA scores and scar improvement rates of V-shaped (b), U-shaped (c), and M-shaped atrophic acne scars (d). (e) The overall GSS score and scar improvement rate. (f, g) Representative facial images of two cases at baseline and 4 weeks after the final treatment. \* $p < 0.05$  vs. FCL + NC group; PT, post-treatment.

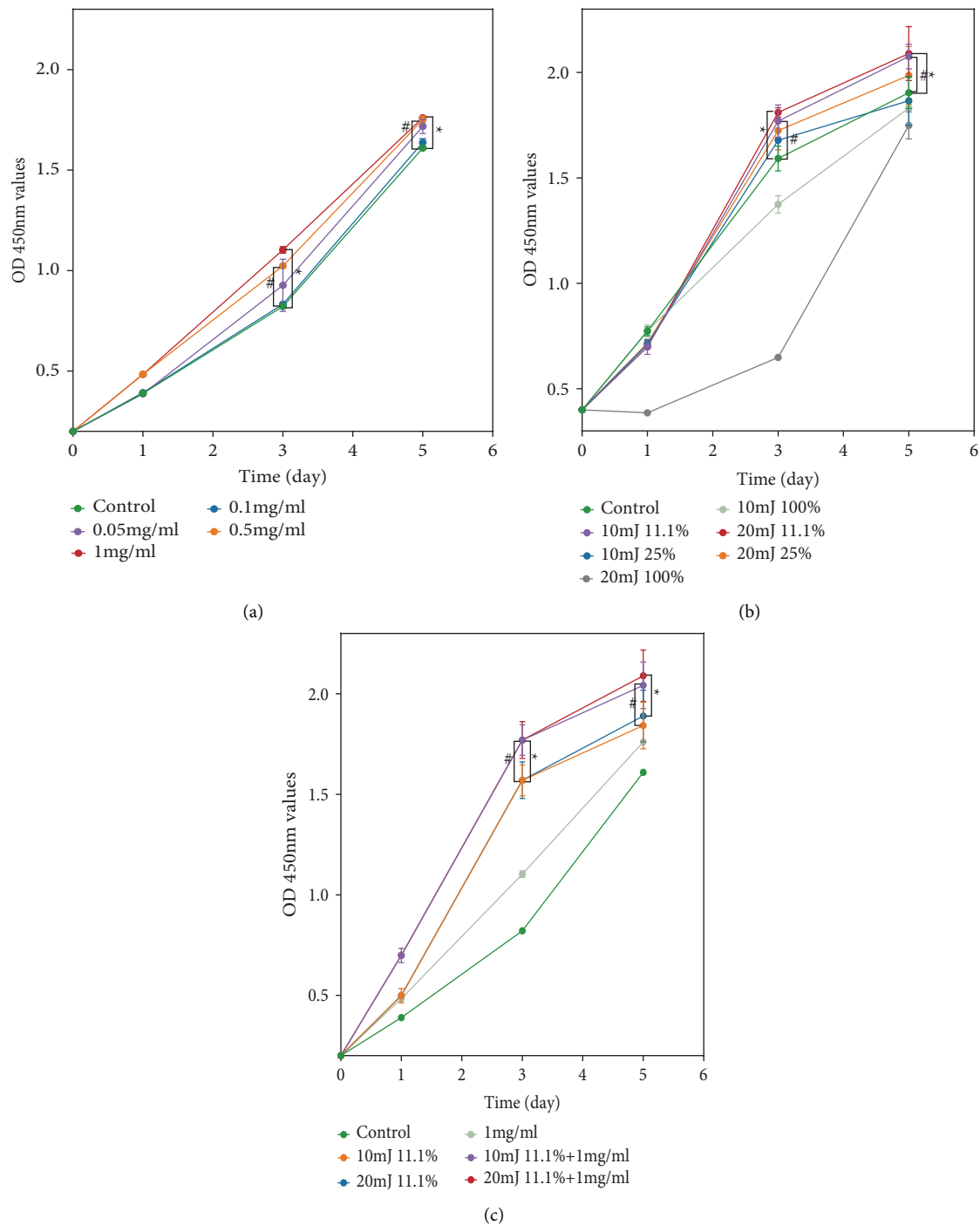


FIGURE 3: FCL combined with rhCol III promotes the proliferation of HDFs in vitro. (a) Cell viability of HDFs induced with 0.05, 0.1, 0.5, and 1 mg/mL rhCol III. (b) Cell viability of HDFs induced with 10, and 20 mJ FCL at a density of 11.1%, 25%, and 100%. (c) Cell viability of HDFs co-induced with 1 mg/mL rhCol III combined with 10, and 20 mJ FCL at a density of 11.1%. \* $p < 0.05$  vs. control.

protein-protein interaction (PPI) network with the betweenness centrality (BC) scores was visualized by CytoNCA, presenting the top five genes with the highest BC scores as *FOS*, *NFKB1*, *IL1B*, *MAP2K3*, and *SRF* (Figure 6(c),6(d)).

Additionally, DEGs between the FCL + rhCol III group and FCL group were mainly enriched in cell division, DNA damage response, positive regulation of cell

population proliferation, cell cycle, and cellular response to mechanical stimulus (Figure 6(e)). Significantly enriched signaling pathways included the cell cycle and cytokine-cytokine receptor interaction (Figure 6(f)). Visualized in the PPI network involving DEGs associated with cell cycle, the top five key genes with the highest BC scores were the *CDK2*, *CCNA2*, *CDK1*, *CCNB1*, and *CDC20* (Figure 6(g),6(h)).

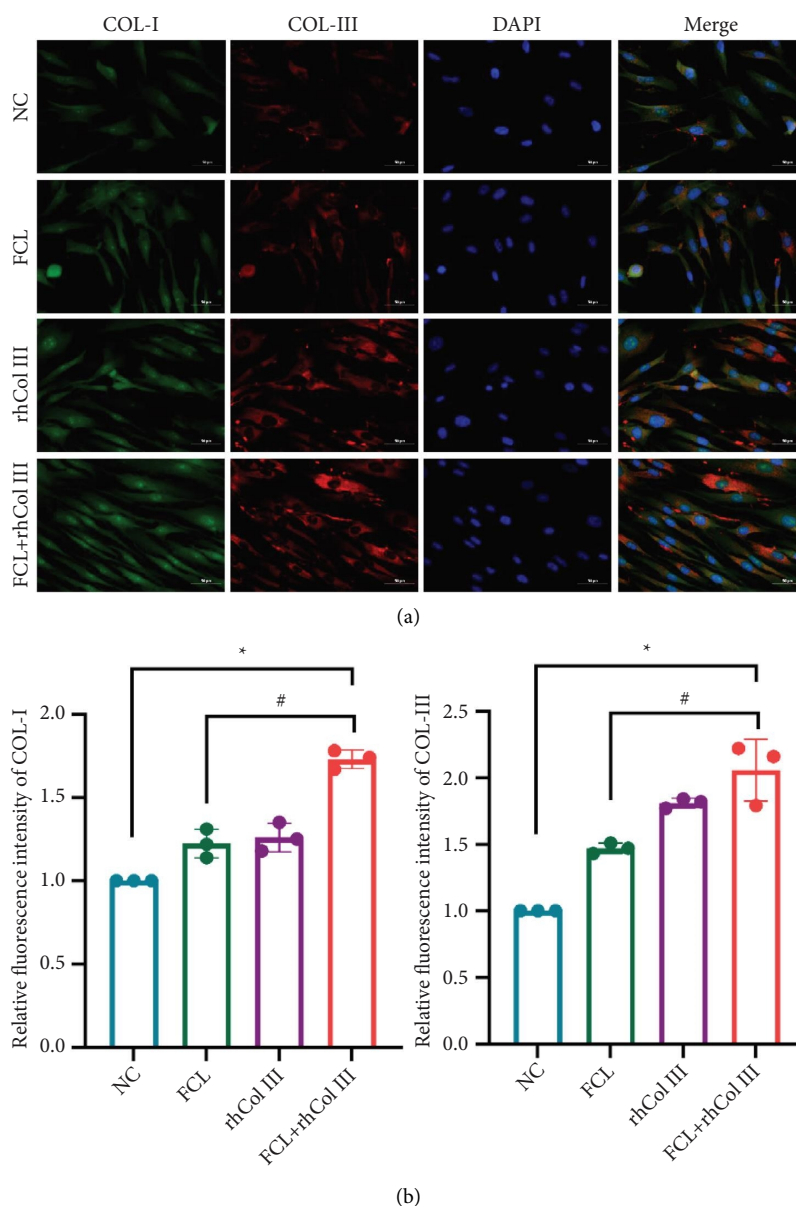


FIGURE 4: FCL combined with rhCol III upregulates type I and III collagens in HDFs in vitro. (a) Immunofluorescence staining of type I and III collagens in HDFs. Scale bar = 50  $\mu$ m,  $n = 3$ . (b) Quantitative analysis of the immunofluorescence intensities of type I and III collagens. \* $p < 0.05$  vs. NC group; # $p < 0.05$  vs. FCL group.

Finally, a Venn diagram visualized an intersection between the rhCol III and NC groups, and those between the FCL + rhCol III and FCL groups, consisting of 445 key DEGs (Figure 7(a)). They were primarily involved in the innate immune response, positive regulation of the MAPK cascade, negative regulation of the apoptotic process, positive regulation of gene expression, and cell division (Figure 7(b)). The MAPK pathway was the dominant one enriched in the key DEGs (Figure 7(c)). The PPI network illustrated that the following regulatory genes were involved in the MAPK pathway enriched in the key DEGs: the *FOS*, *NFKB1*, *IL1B*, *SRF*, *KDR*, *FGF10*, *FGF18*, *FGF22*, *RASA1*, and *BDNF* genes (Figure 7(d),7(e)).

#### 4. Discussion

FCL has been established for its efficacy in treating acne atrophic scarring; however, not all types of acne scars can benefit entirely from a single treatment. Our study demonstrated the effectiveness of combining FCL with rhCol III in expediting the repair and remodeling of skin tissue to diminish atrophic acne scars. The mechanism behind this involves the regulation of cell proliferation and collagen synthesis through the MAPK signaling pathway.

Especially in treating boxcar and icepick scars, we have consistently observed that a combination treatment of FCL with other therapeutic approaches offers a more favorable

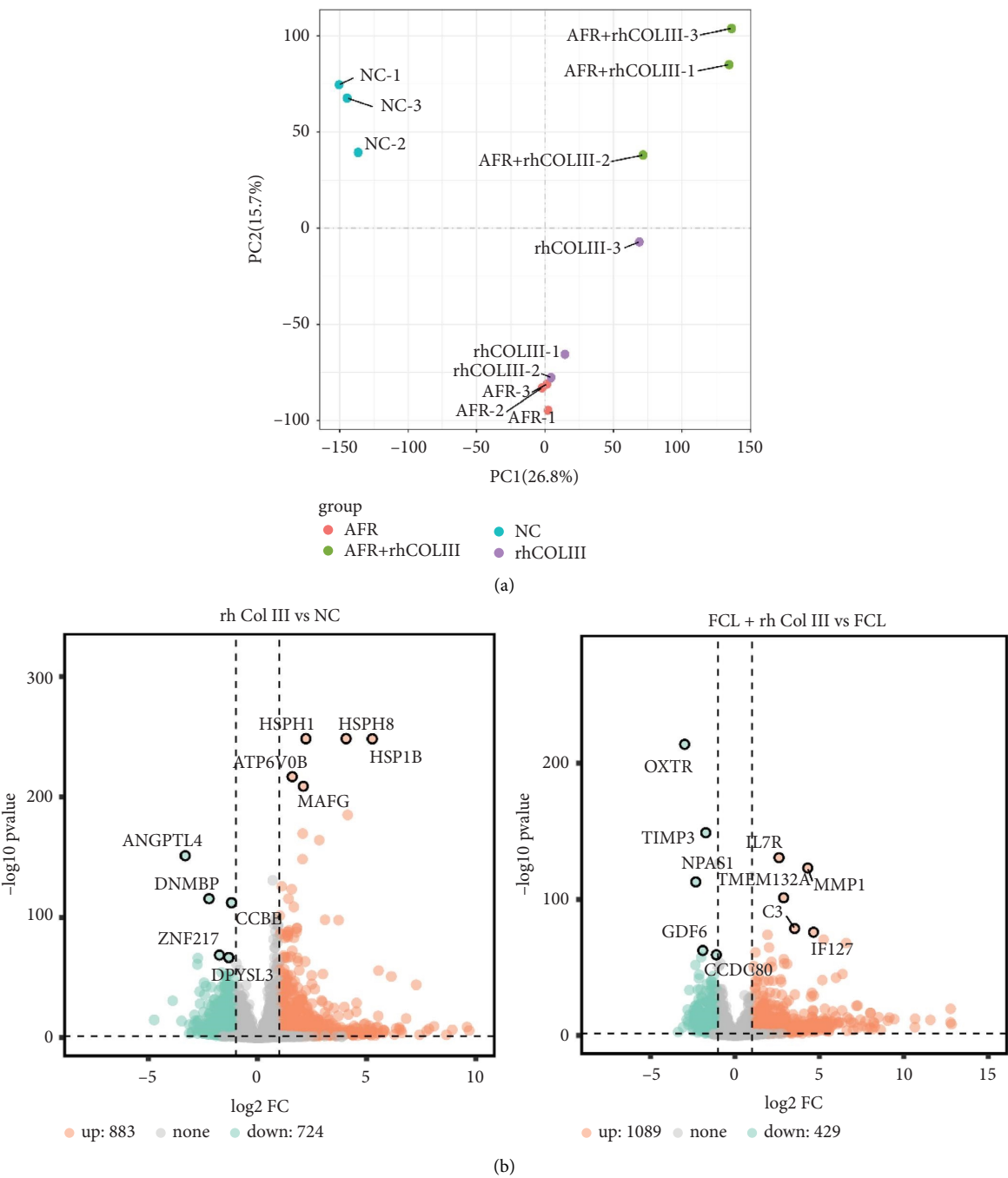
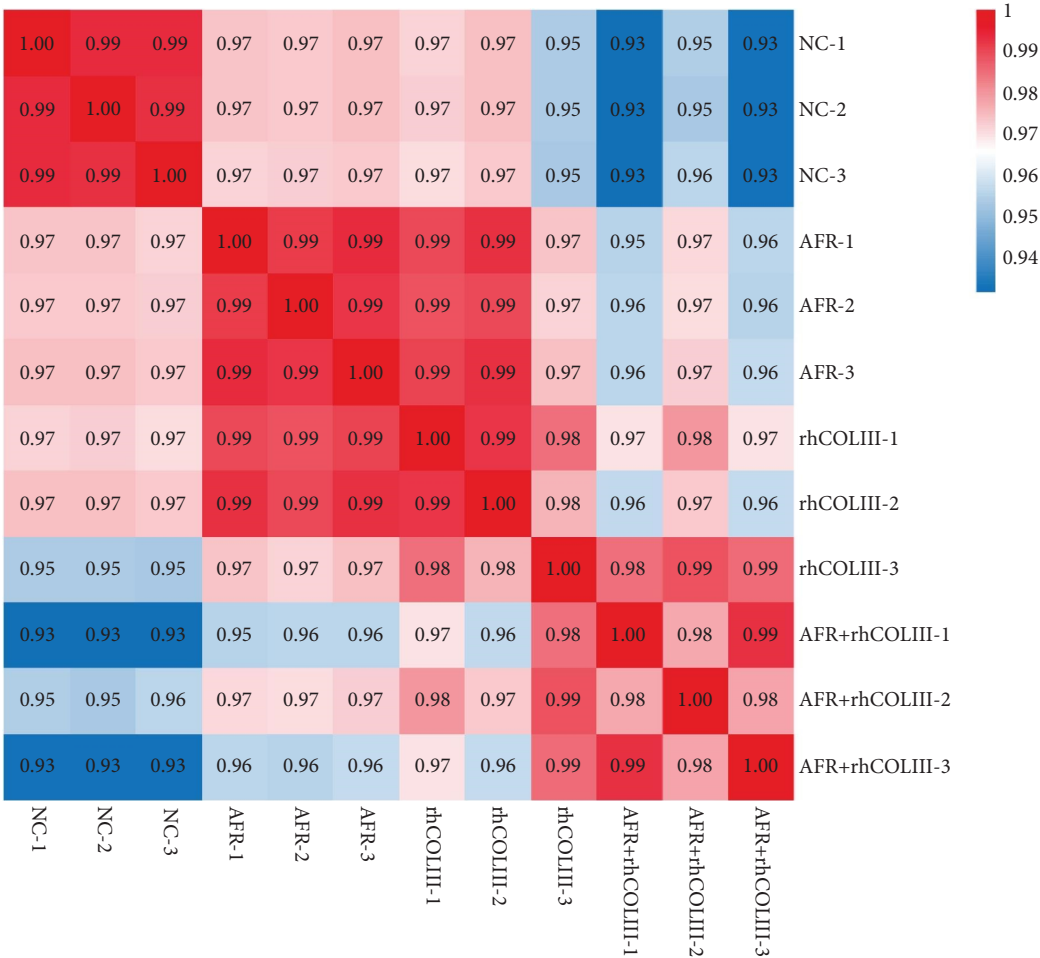


FIGURE 5: Continued.



(c)  
FIGURE 5: Continued.

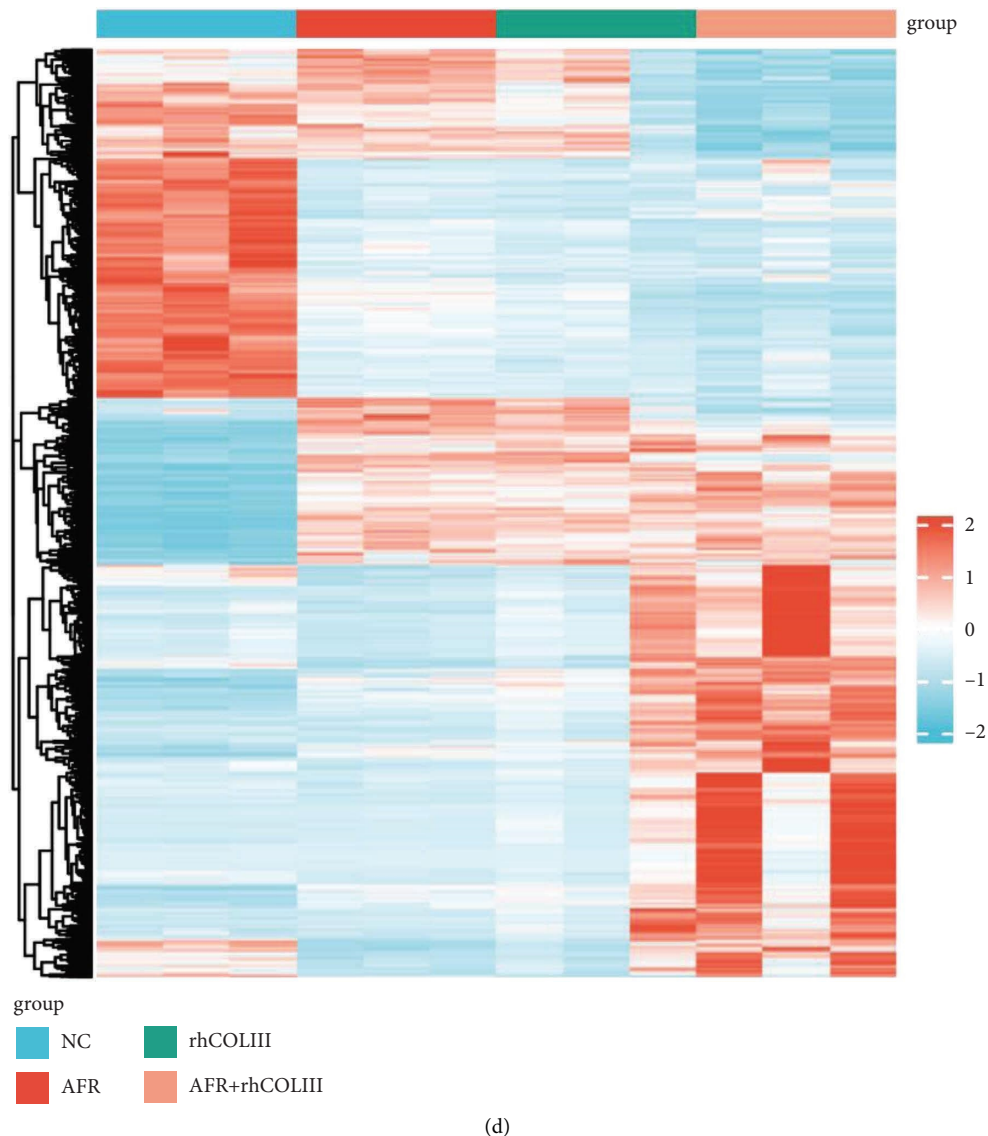


FIGURE 5: Identification of DEGs in HDFs co-induced with FCL and rhCol III. (a) Scatterplots of the principal component analysis (PCA). (b) Volcano plots of DEGs, with green dots representing downregulated and red dots indicating upregulated ones. (c) A correlation heatmap. (d) A clustering heatmap. NC, NC group; AFR, FCL group; AFR + rhCol III, FCL + rhCol III group.

outcome than laser monotherapy [17]. Similar evidence also points out that FCL alone is less effective in treating icepick scars [11, 18]. With its shallow penetration (2–4 mm depth) [11], FCL can hardly treat icepick scars, which are typically manifested as narrow openings and deep extensions into the dermis or even subcutaneous tissue [19, 20]. Synergistically, rhCol III injections assist FCL in overcoming its drawbacks by stimulating the repair of deeper dermal tissues.

FCL aims to stimulate collagen production and remodeling through various methods, thereby improving facial appearance in atrophic scars via a microexfoliation effect [21]. In contrast, rhCol III plays a role in skin tissue repair through multiple mechanisms. Initially, rhCol III enhances the regulation of ECM remodeling. Li et al. [22] showed that local injections of rhCol III promote the synthesis of type I and III collagens, thereby restoring the

arrangement of myofibrils and collagen structures in rats with pelvic floor dysfunction. Both *in vivo* and *in vitro* studies have confirmed the role of rhCol III in facilitating collagen deposition and angiogenesis around the injection site. Wang et al. [14] indicated that an intradermal injection of rhCol III significantly increases the thickness of both the epidermis and dermis in rats with UV-induced skin photoaging by upregulating type I and III collagens. Secondly, rhCol III activates key reparative cells, such as fibroblasts and epidermal cells, to promote tissue reconstruction. Dong et al. revealed the excellent biocompatibility and strong cell-adhering properties of rhCol III, which favor the adhesion and migration of fibroblasts and epidermal cells [23]. Additionally, rhCol III provides an ideal microenvironment for fibroblasts to initiate cell adhesion [14]. Lastly, rhCol III alleviates inflammatory responses by inhibiting macrophage



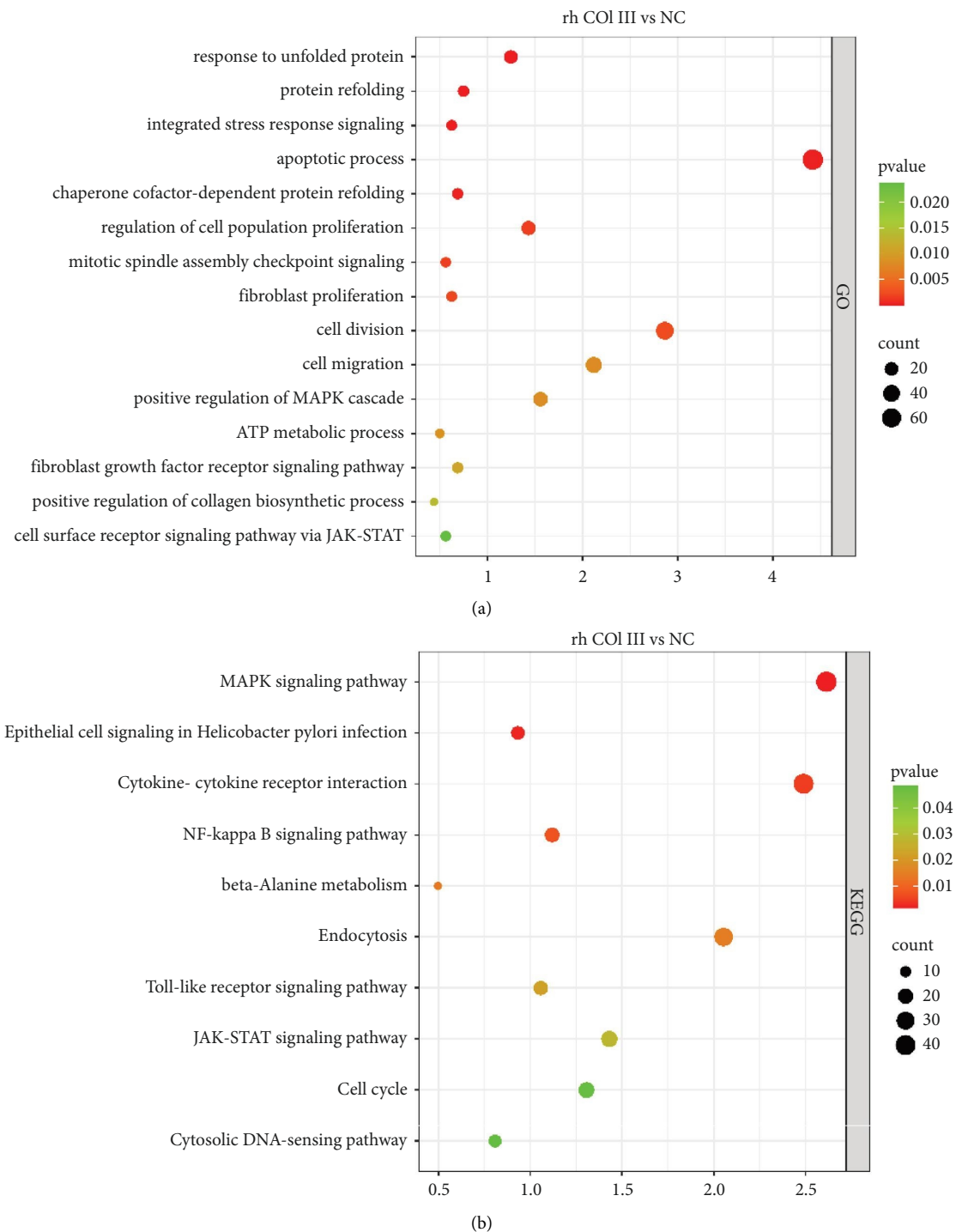


FIGURE 6: Continued.

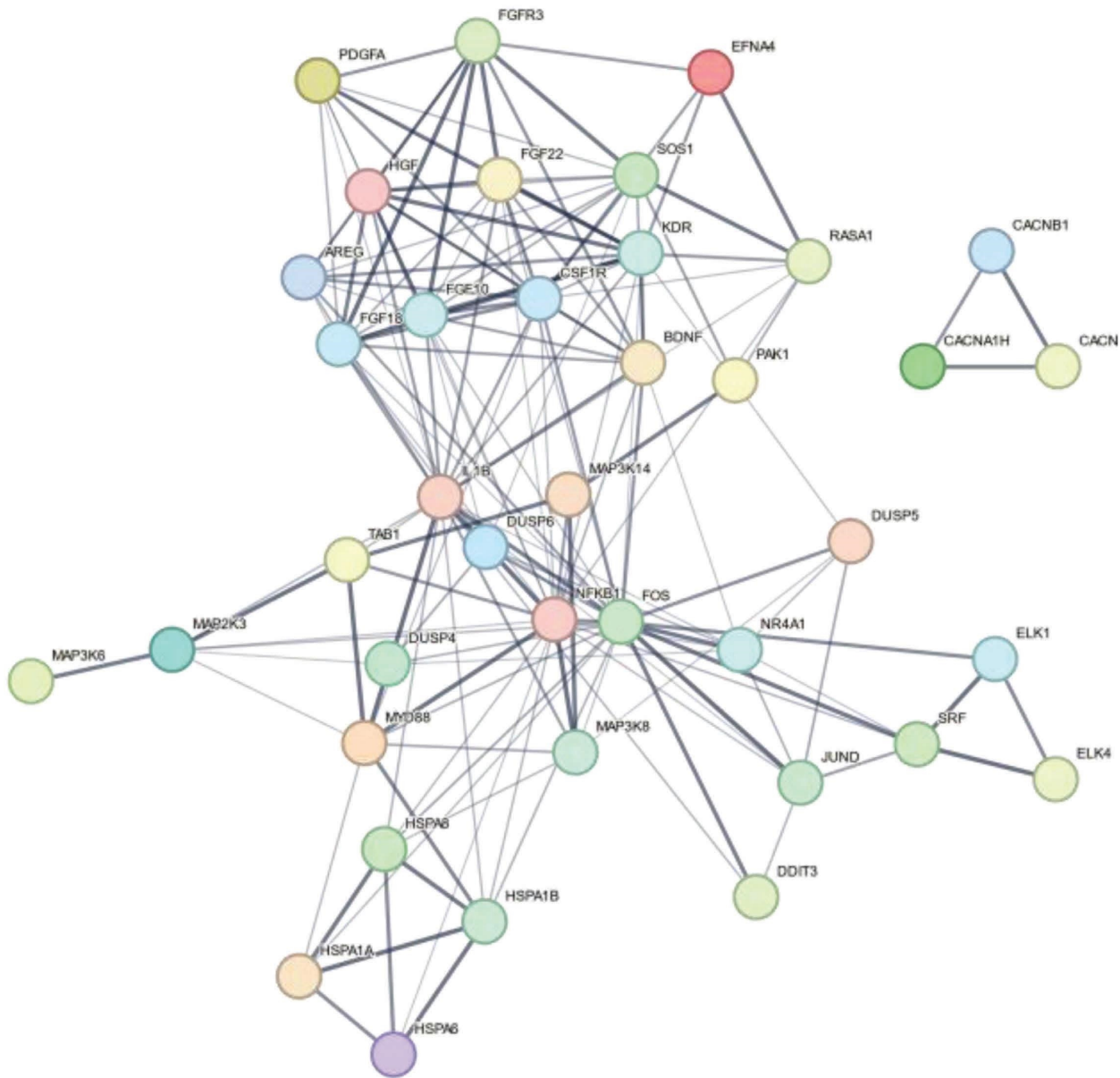
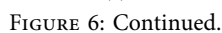
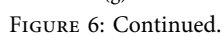


FIGURE 6: Continued.







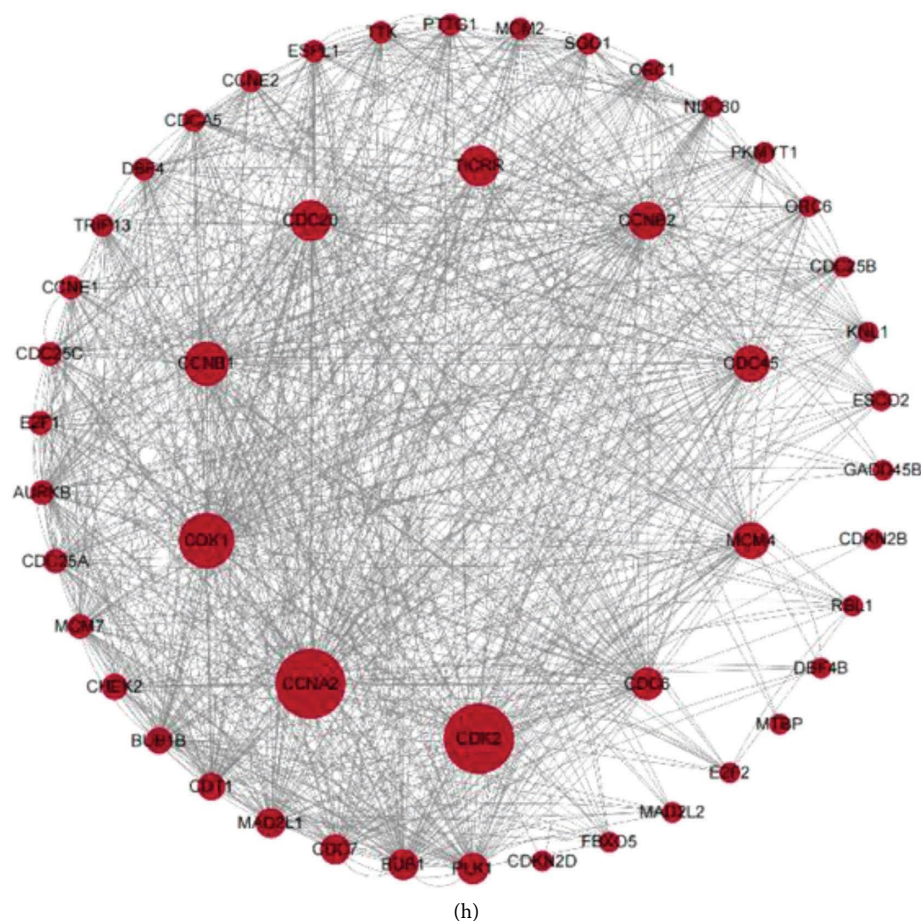


FIGURE 6: GO/KEGG enrichment analyses. (a, b) GO (a) and KEGG (b) enrichment analyses of DEGs between the rhCol III and NC groups. (c) A PPI network of DEGs between the rhCol III and NC groups. (d) Key genes in the PPI, where nodes represent proteins, and connectors represent protein-associated roles. The color intensity indicates the p-adjust value of the corresponding GO term, and the bubble size represents the number of query genes in the gene set associated with the given GO term. (e, f) GO (e) and KEGG (f) enrichment analyses of DEGs between the FCL + rhCol III and FCL groups. (g) A PPI network of DEGs between the FCL + rhCol III and FCL groups. (h) Key genes in the PPI. DEGs, differentially expressed genes; GO, Gene Ontology; KEGG, Kyoto Encyclopedia of Genes and Genomes; PPI, protein-protein interaction.

aggregation [24]. Although rhCol III suppresses the expressions of inflammatory factors (e.g., IL-1 $\beta$  and TNF- $\alpha$ ) during the treatment of oral ulcers, its anti-inflammatory property contributes only marginally to early healing [12]. In our study, we consistently observed higher positive expressions of type I and III collagens in HDFs induced with FCL combined with rhCol III than in those induced with FCL alone.

RNA-seq and bioinformatics revealed the molecular mechanisms of FCL combined with rhCol III in treating acne scars. Notably, the MAPK signaling pathway was the most significantly enriched one in the DEGs we identified. The MAPK signaling pathway is extensively involved in cell proliferation, migration, inflammatory response, and ECM remodeling [25]. Phimmuan et al. [26] demonstrated that the application of  $\gamma$ -irradiated blended fibroin/aloe gel accelerates skin wound healing by increasing the secretion of vascular endothelial growth factor via the MAPK/ERK signaling pathway. Ononin modulates the inflammatory response and ECM by activating the MAPK pathway [27].

ERK1/2 is a member of the MAPKs activated to promote fibroblast proliferation and migration [28, 29]. The ERK signaling pathway is responsible for driving the production of ECM-related proteins [30, 31]. Here, we identified 10 key genes associated with the MAPK signaling pathway, including *FOS*, *NFKB1*, *IL1B*, *SRF*, *KDR*, *FGF10*, *FGF18*, *FGF22*, *RASA1*, and *BDNF*. Among them, *FOS* plays a crucial role in cell growth and differentiation [32]. FGF10 is a member of the FGF family that regulates fibroblast proliferation, differentiation, and ECM production by activating the MAPK pathway [32, 33]. FGF18 can accelerate articular cartilage repair and promote tissue healing [34]. Overall, we believe that the MAPK signaling pathway and the key downstream genes were main characters underlying the efficacy of FCL combined with rhCol III in treating atrophic acne scars.

Recent years have witnessed a surge in research on the application of FCL combination therapy for acne scarring. Zhang et al. discovered that combining 30% salicylic acid with FCL results in superior prevention and alleviation of

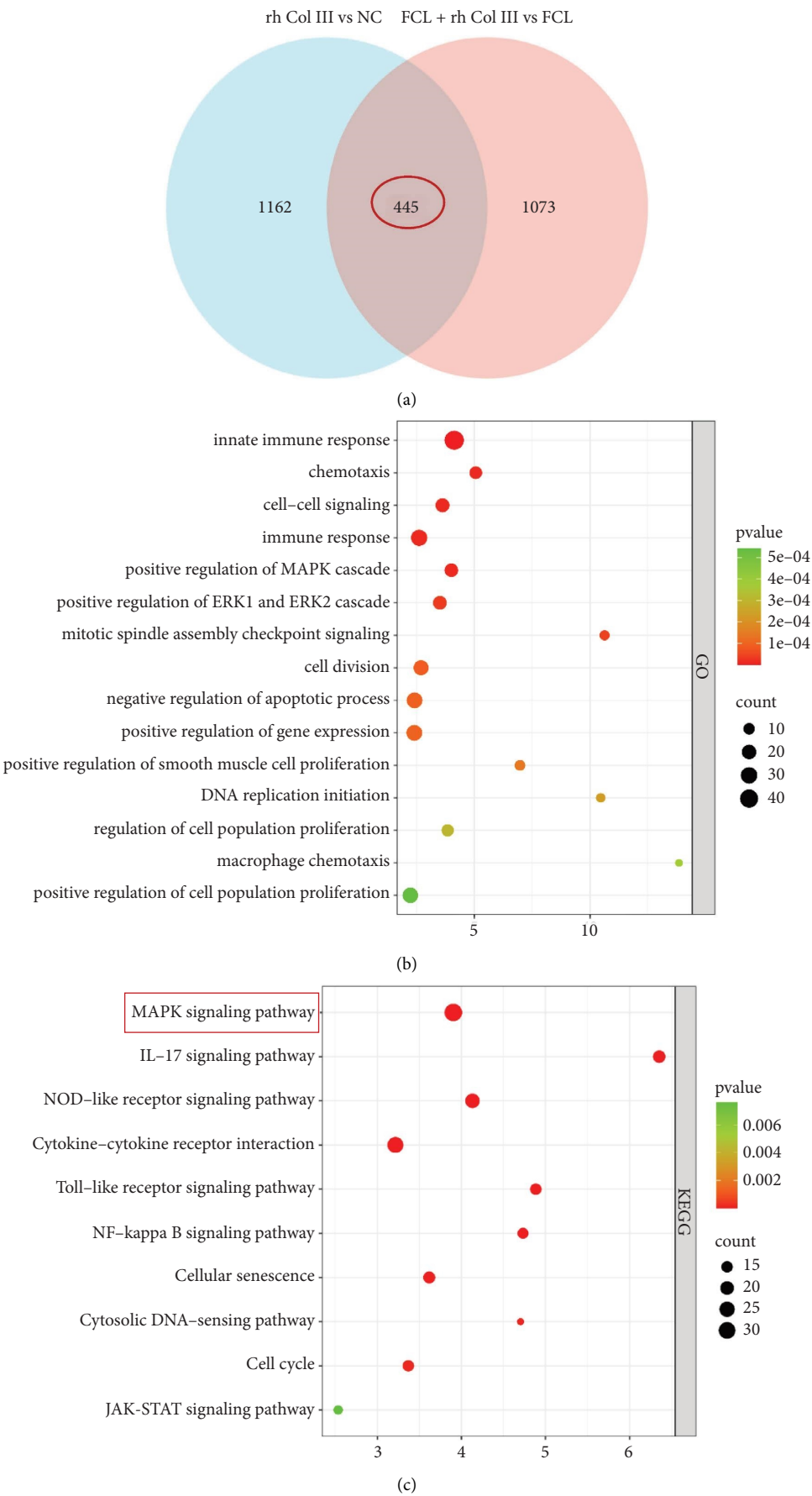
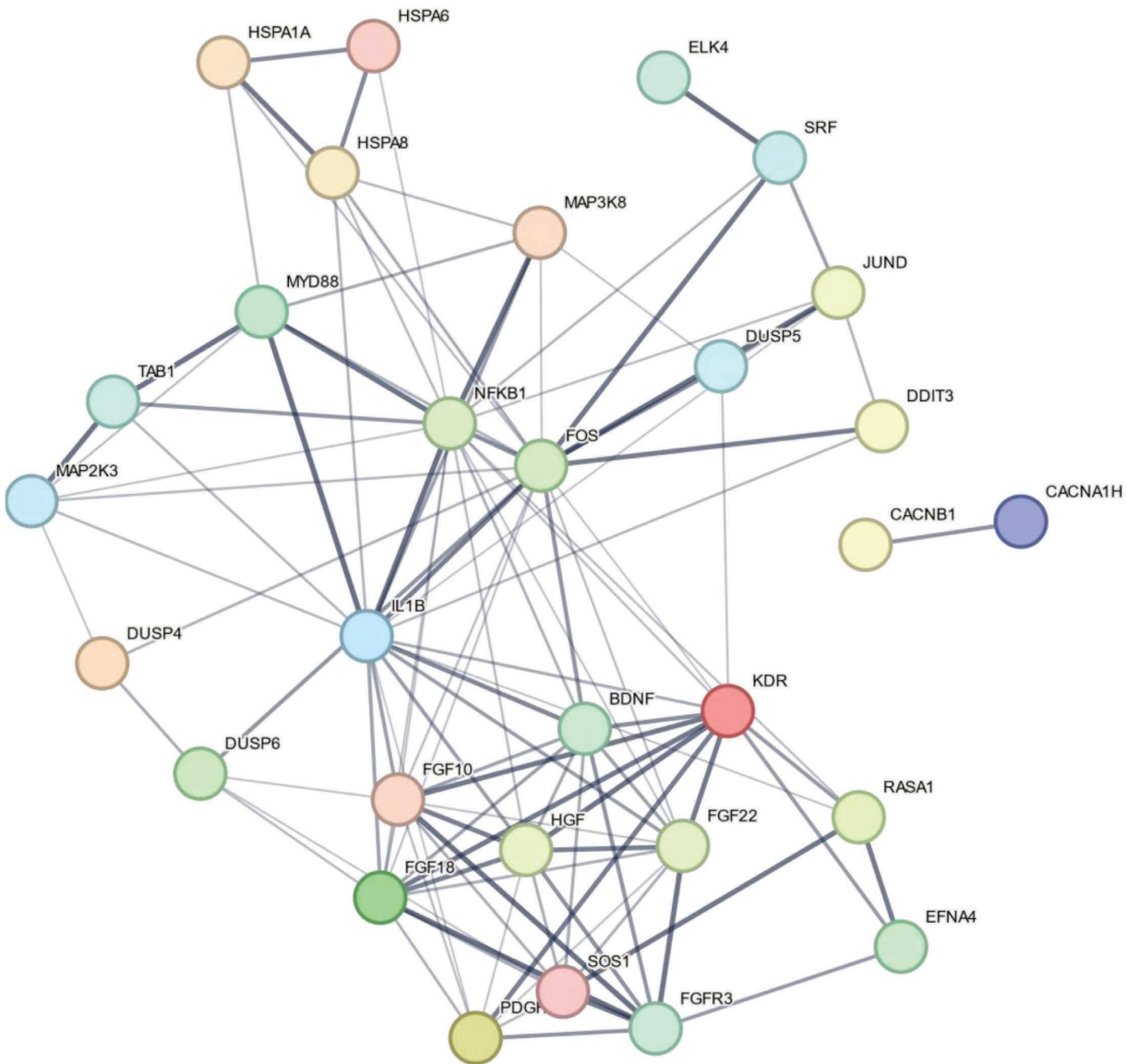


FIGURE 7: Continued.



(d)  
FIGURE 7: Continued.



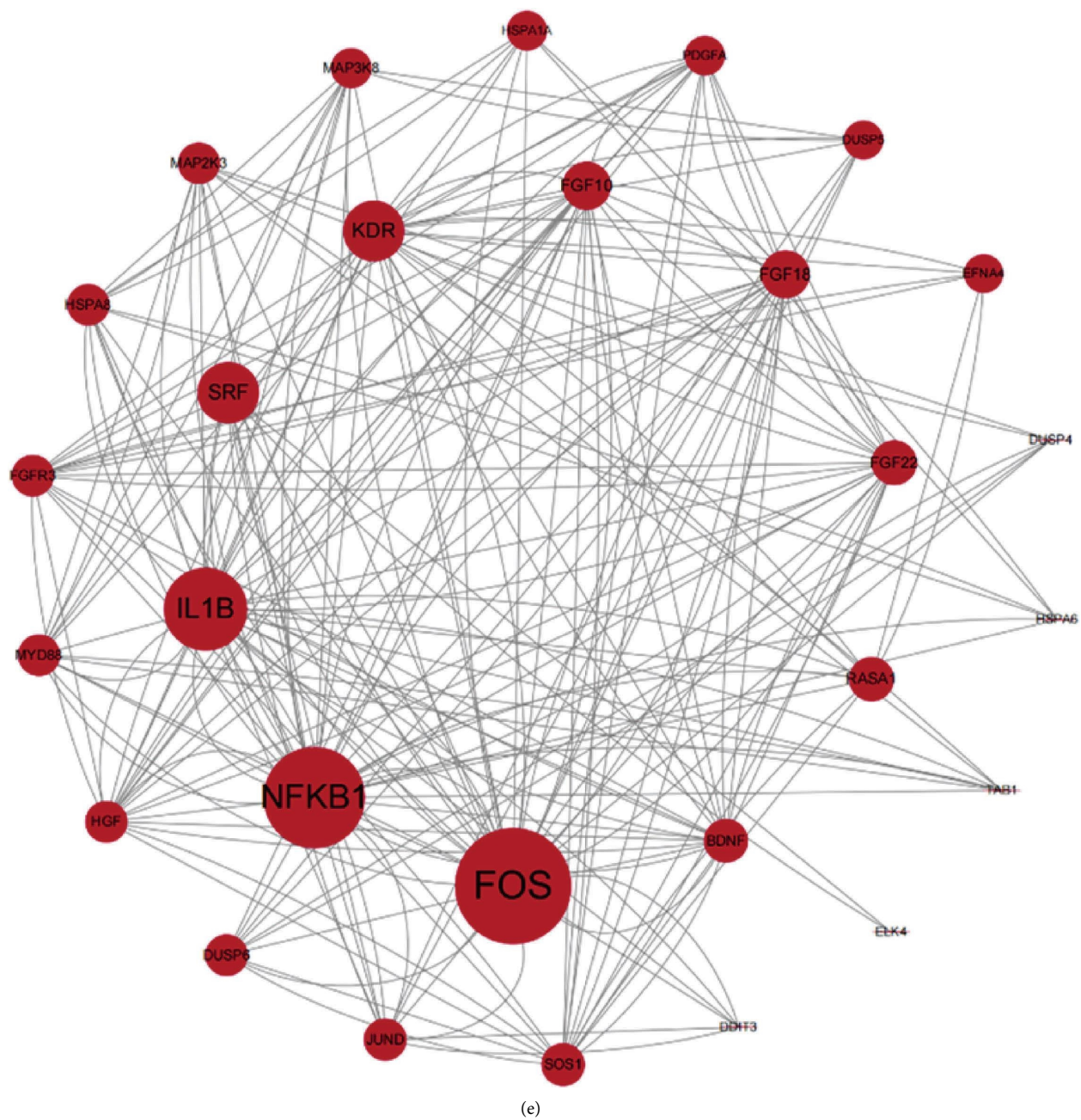


FIGURE 7: DEGs and molecular functions responsible for the efficacy of FCL combined with rhCol III in treating acne scars. (a) A Venn diagram illustrating the intersection of DEGs between rhCol III versus NC and FCL + rhCol III versus FCL. (b, c) GO (b) and KEGG (c) enrichment analyses of intersected DEGs. (d) A PPI network of intersected DEGs. (e) Key genes identified using the CytoHubba plugin.

acne scars by inhibiting inflammatory factors [21]. Kwon et al. [35] demonstrated that FCL enhances the local diffusion of adipose-derived stem cells, ultimately leading to a synergistic effect of rapid healing. Abdel-Maguid et al. [36] also showed that the combination of amniotic fluid-derived stem cell-conditioned medium (AFSC-CM) and platelet-rich plasma (PRP) with FCL significantly activates fibroblast proliferation and differentiation, as well as stimulates ECM production and remodeling. The combination of FCL and hyaluronic acid dressing yields satisfactory outcomes by promoting tissue remodeling and angiogenesis [3]. In the

present study, dermal injections of rhCol III synergistically assisted FCL in treating acne scars, achieving stronger efficacy than FCL monotherapy.

Limitations of the study should be considered. First, it was a small-scale study lacking a long-term follow-up. Second, efficacy assessments by physicians from the two medical institutions may produce biases. Third, how the MAPK signaling pathway exactly mediates scar repair remains to be further explored in vitro. Fourth, the current study focused primarily on the MAPK signaling pathway, without comprehensive investigation into other potential

signaling mechanisms that may also be involved in scar repair. Fifth, the patient population in this study was relatively homogeneous, which may limit the generalizability of the findings to other diverse populations. Therefore, future studies with larger sample sizes, longer follow-up periods, and more comprehensive assessments of signaling mechanisms are needed to further validate and expand upon the findings of this study.

In conclusion, the combination of FCL and rhCol III has shown encouraging efficacy and safety in treating facial atrophic acne scars. Additionally, rhCol III has provided a synergistic effect on FCL by promoting skin cell regeneration and ECM remodeling through the MAPK signaling pathway.

## Data Availability Statement

The data that support the findings of this study are available from the corresponding authors upon reasonable request.

## Ethics Statement

The study was conducted in accordance with the Declaration of Helsinki and was approved by the Ethics Committee of Nantong Third People's Hospital (No: EL2022007), the Ethics Committee of Nanjing Yijia Medical Aesthetic Clinic (No: 2022-10-10), and the Ethics Committee of Taiyuan Vitiligo Hospital (No: 2022001).

## Consent

Informed consent was received from all participants.

## Disclosure

All authors have approved the submission of this manuscript. All content was solely prepared by the human authors.

## Conflicts of Interest

The authors acknowledge the provision of rhCol III for this research from Shanxi Jinbo Biomedical Co., Ltd. The sponsor was not involved in the study design; in the collection, analysis, or interpretation of data; in the writing of the manuscript; or in the decision to publish the results. The content is solely the responsibility of the authors.

## Author Contributions

Conceived and designed the experiments: Li Gu, Jing Wang, Rong Guo, Bingrong Zhou, Hui Hua. Performed experiments: Li Gu, Jing Wang. The data analysis was performed by Jing Wang. All statistical analyses were performed by Jing Wang, an experienced researcher in biostatistics. Contributed reagents/materials/analysis tool: Zhinan Shi, Zhiyi Xu, Shu Zhou, Jingting Zhao. Investigation: Liqun Gu. Review and editing: Bingrong Zhou, Hui Hua. Writing: Li Gu, Jing Wang. Li Gu, Jing Wang and Rong Guo contributed equally.

## Funding

This work was supported by the National Natural Science Foundation of China (No. 82073472), Nantong University Special Research Fund for Clinical Medicine (No. 2024JZ021), Nantong University Special Research Fund for Clinical Medicine (No. 2024LQ041), and the Nantong Young Medical Key Talent Program.

## Acknowledgments

No generative AI was used in the preparation of this manuscript.

## References

- [1] Z. Ding, Z. Pan, Y. Tang, et al., "Effectiveness and Safety of the Modified Multiple Mode Procedures Versus Traditional Multiple Mode Procedures on Treating Facial Atrophic Acne Scars: a Propensity Score Matching Retrospective Cohort Study," *Lasers in Medical Science* 39, no. 1 (2024): 260, <https://doi.org/10.1007/s10103-024-04211-y>.
- [2] J. Tan, S. Kang, and J. Leyden, "Prevalence and Risk Factors of Acne Scarring Among Patients Consulting Dermatologists in the USA," *Journal of Drugs in Dermatology* 16, no. 2 (2017): 97–102.
- [3] J. Zhang, F. Xu, H. Lin, et al., "Efficacy of Fractional CO(2) Laser Therapy Combined with Hyaluronic Acid Dressing for Treating Facial Atrophic Acne Scars: A Systematic Review and Meta-Analysis of Randomized Controlled Trials," *Lasers in Medical Science* 38, no. 1 (2023): 214, <https://doi.org/10.1007/s10103-023-03879-y>.
- [4] F. Salameh, P. R. Shumaker, G. J. Goodman, et al., "Energy-Based Devices for the Treatment of Acne Scars: 2022 International Consensus Recommendations," *Lasers in Surgery and Medicine* 54, no. 1 (2022): 10–26, <https://doi.org/10.1002/lsm.23484>.
- [5] J. Tan, S. Beissert, F. Cook-Bolden, et al., "Impact of Facial Atrophic Acne Scars on Quality of Life: A Multi-Country Population-Based Survey," *American Journal of Clinical Dermatology* 23, no. 1 (2022): 115–123, <https://doi.org/10.1007/s40257-021-00628-1>.
- [6] Z. Ding, Y. Guo, Y. Guo, et al., "Efficacy and Safety of Fractional Microneedle Radiofrequency for Atrophic Acne Scars: A real-world Clinical Study of 126 Patients," *Lasers in Surgery and Medicine* 56, no. 2 (2024): 150–164, <https://doi.org/10.1002/lsm.23759>.
- [7] Y. E. Aljefri, A. A. Ghaddaf, R. A. Alahmadi, et al., "Ablative Fractional Carbon Dioxide Laser Combined with Autologous Platelet-Rich Plasma in the Treatment of Atrophic Acne Scars: A Systematic Review and Meta-Analysis," *Dermatologic Therapy* 35, no. 12 (2022): e15888, <https://doi.org/10.1111/dth.15888>.
- [8] M. Boen and C. Jacob, "A Review and Update of Treatment Options Using the Acne Scar Classification System," *Dermatologic Surgery* 45, no. 3 (2019): 411–422, <https://doi.org/10.1097/dss.0000000000001765>.
- [9] Y. Z. Mu, L. Jiang, and H. Yang, "The Efficacy of Fractional Ablative Carbon Dioxide Laser Combined with Other Therapies in Acne Scars," *Dermatologic Therapy* 32, no. 6 (2019): e13084, <https://doi.org/10.1111/dth.13084>.
- [10] H. Schwaiger, M. Heppt, J. Poetschke, et al., "Comparison of Two Kinds of Lasers in the Treatment of Acne Scars," *Facial*

- Plastic Surgery* 31, no. 05 (2015): 523–531, <https://doi.org/10.1055/s-0035-1567814>.
- [11] Z. Pan, Y. Tang, H. Hua, Z. Hou, and B. Zhou, “Multiple Mode Procedures of Ultra-Pulse Fractional CO(2) Laser: A Novel Treatment Modality of Facial Atrophic Acne Scars,” *Journal of Clinical Medicine* 12, no. 13 (2023): 4388, <https://doi.org/10.3390/jcm12134388>.
  - [12] X. Shuai, N. Kang, Y. Li, et al., “Recombination Humanized Type III Collagen Promotes Oral Ulcer Healing,” *Oral Diseases* 30, no. 3 (2024): 1286–1295, <https://doi.org/10.1111/odi.14540>.
  - [13] L. Y. Long, W. Liu, L. Li, et al., “Dissolving Microneedle-Encapsulated Drug-Loaded Nanoparticles and Recombinant Humanized Collagen Type III for the Treatment of Chronic Wound via Anti-Inflammation and Enhanced Cell Proliferation and Angiogenesis,” *Nanoscale* 14, no. 4 (2022): 1285–1295, <https://doi.org/10.1039/d1nr07708b>.
  - [14] J. Wang, H. Qiu, Y. Xu, et al., “The Biological Effect of Recombinant Humanized Collagen on Damaged Skin Induced by UV-Photoaging: An in Vivo Study,” *Bioactive Materials* 11 (2022): 154–165, <https://doi.org/10.1016/j.bioactmat.2021.10.004>.
  - [15] S. McLaughlin, B. McNeill, J. Podrebarac, et al., “Injectable Human Recombinant Collagen Matrices Limit Adverse Remodeling and Improve Cardiac Function After Myocardial Infarction,” *Nature Communications* 10, no. 1 (2019): 4866, <https://doi.org/10.1038/s41467-019-12748-8>.
  - [16] J. Wang, L. Gu, Z. Shi, et al., “5-Aminolevulinic Acid Photodynamic Therapy Protects Against UVB-Induced Skin Photoaging: A DNA-Repairing Mechanism Involving the BER Signalling Pathway,” *Journal of Cellular and Molecular Medicine* 28, no. 14 (2024): e18536, <https://doi.org/10.1111/jcmm.18536>.
  - [17] Z. A. Ibrahim, A. A. El-Ashmawy, and O. A. Shora, “Therapeutic Effect of Microneedling and Autologous platelet-rich Plasma in the Treatment of Atrophic Scars: a Randomized Study,” *Journal of Cosmetic Dermatology* 16, no. 3 (2017): 388–399, <https://doi.org/10.1111/jocd.12356>.
  - [18] I. Majid and S. Imran, “Fractional CO2 Laser Resurfacing as Monotherapy in the Treatment of Atrophic Facial Acne Scars,” *Journal of Cutaneous and Aesthetic Surgery* 7, no. 2 (2014): 87–92, <https://doi.org/10.4103/0974-2077.138326>.
  - [19] B. Li, K. Ren, X. Yin, H. She, H. Liu, and B. Zhou, “Efficacy and Adverse Reactions of Fractional CO(2) Laser for Atrophic Acne Scars and Related Clinical Factors: A Retrospective Study on 121 Patients,” *Journal of Cosmetic Dermatology* 21, no. 5 (2022): 1989–1997, <https://doi.org/10.1111/jocd.14868>.
  - [20] S. B. Kaushik and A. F. Alexis, “Nonablative Fractional Laser Resurfacing in Skin of Color: Evidence-Based Review,” *J Clin Aesthet Dermatol* 10, no. 6 (2017): 51–67.
  - [21] Y. J. Zhang, Y. M. Chen, X. Y. Shao, et al., “Combination Treatment with 30% Salicylic Acid and Fractional CO(2) Laser for Acne Scars: A 20-Week Prospective, Randomized, Split-Face Study,” *Dermatologic Therapy* 35, no. 9 (2022): e15693, <https://doi.org/10.1111/dth.15693>.
  - [22] H. Li, S. You, X. Yang, S. Liu, and L. Hu, “Injectable Recombinant Human Collagen-Derived Material with High Cell Adhesion Activity Limits Adverse Remodelling and Improves Pelvic Floor Function in Pelvic Floor Dysfunction Rats,” *Biomaterials Advances* 134 (2022): 112715, <https://doi.org/10.1016/j.msec.2022.112715>.
  - [23] Z. Dong, Q. Liu, X. Han, et al., “Electrospun Nanofibrous Membranes of Recombinant Human Collagen Type III Promote Cutaneous Wound Healing,” *Journal of Materials Chemistry B* 11, no. 27 (2023): 6346–6360, <https://doi.org/10.1039/d3tb00438d>.
  - [24] C. Hu, W. Liu, L. Long, et al., “Microenvironment-Responsive Multifunctional Hydrogels with Spatiotemporal Sequential Release of Tailored Recombinant Human Collagen Type III for the Rapid Repair of Infected Chronic Diabetic Wounds,” *Journal of Materials Chemistry B* 9, no. 47 (2021): 9684–9699, <https://doi.org/10.1039/d1tb02170b>.
  - [25] Q. Gan, X. Huang, W. Zhao, et al., “AC010883.5 Promotes Cell Proliferation, Invasion, Migration, and Epithelial-to-Mesenchymal Transition in Cervical Cancer by Modulating the MAPK Signaling Pathway,” *BMC Cancer* 23, no. 1 (2023): 364, <https://doi.org/10.1186/s12885-023-10825-2>.
  - [26] P. Phimmuan, Z. Dirand, M. Tissot, et al., “Beneficial Effects of a Blended Fibroin/Aloe Gel Extract Film on the Biomolecular Mechanism(S) via the MAPK/ERK Pathway Relating to Diabetic Wound Healing,” *ACS Omega* 8, no. 7 (2023): 6813–6824, <https://doi.org/10.1021/acsomega.2c07507>.
  - [27] F. Xu, L. J. Zhao, T. Liao, et al., “Ononin Ameliorates Inflammation and Cartilage Degradation in Rat Chondrocytes with IL-1 $\beta$ -Induced Osteoarthritis by Downregulating the MAPK and NF- $\kappa$ B Pathways,” *BMC Complement Med Ther* 22, no. 1 (2022): 25, <https://doi.org/10.1186/s12906-022-03504-5>.
  - [28] Y. Zhang, S. Li, H. Chen, et al., “Non-Genomic Mechanisms Mediate Androgen-Induced PSD95 Expression,” *Aging* 11, no. 8 (2019): 2281–2294, <https://doi.org/10.18632/aging.101913>.
  - [29] K. Imoto, M. Okada, and H. Yamawaki, “Periostin Mediates Right Ventricular Failure Through Induction of Inducible Nitric Oxide Synthase Expression in Right Ventricular Fibroblasts from Monocrotaline-Induced Pulmonary Arterial Hypertensive Rats,” *International Journal of Molecular Sciences* 20, no. 1 (2018): 62, <https://doi.org/10.3390/ijms20010062>.
  - [30] M. J. Yim, J. M. Lee, S. C. Ko, et al., “Antifibrosis Efficacy of Apo-9-Fucoxanthinone-Contained Sargassum horneri Ethanol Extract on Nasal Polyp: an in Vitro and Ex Vivo Organ Culture Assay,” *Current Issues in Molecular Biology* 44, no. 11 (2022): 5815–5826, <https://doi.org/10.3390/cimb44110395>.
  - [31] R. K. Bhogal and C. A. Bona, “Regulatory Effect of Extracellular Signal-Regulated Kinases (ERK) on Type I Collagen Synthesis in Human Dermal Fibroblasts Stimulated by IL-4 and IL-13,” *International Reviews of Immunology* 27, no. 6 (2008): 472–496, <https://doi.org/10.1080/08830180802430974>.
  - [32] Y. Dou, Y. Wei, Z. Zhang, et al., “Transcriptome-Wide Analysis of RNA m(6)A Methylation Regulation of Muscle Development in Queshan Black Pigs,” *BMC Genomics* 24, no. 1 (2023): 239, <https://doi.org/10.1186/s12864-023-09346-w>.
  - [33] H. Wang, X. Wang, M. Li, S. Wang, Q. Chen, and S. Lu, “Identification of Key Sex-Specific Pathways and Genes in the Subcutaneous Adipose Tissue from Pigs Using WGCNA Method,” *BMC Genom Data* 23, no. 1 (2022): 35, <https://doi.org/10.1186/s12863-022-01054-w>.
  - [34] X. Chen, A. Yamashita, M. Morioka, et al., “Integration Capacity of Human Induced Pluripotent Stem Cell-Derived Cartilage,” *Tissue Engineering Part A* 25, no. 5-6 (2019): 437–445, <https://doi.org/10.1089/ten.tea.2018.0133>.

- [35] H. H. Kwon, S. H. Yang, J. Lee, et al., "Combination Treatment with Human Adipose Tissue Stem Cell-Derived Exosomes and Fractional CO<sub>2</sub> Laser for Acne Scars: A 12-week Prospective, Double-Blind, Randomized, Split-Face Study," *Acta Dermato-Venereologica* 100, no. 18 (2020): adv00310, <https://doi.org/10.2340/00015555-3666>.
- [36] E. M. Abdel-Maguid, S. M. Awad, Y. S. Hassan, M. A. El-Mokhtar, H. E. El-Deek, and M. M. Mekkawy, "Efficacy of Stem Cell-Conditioned Medium vs. Platelet-Rich Plasma as an Adjuvant to Ablative Fractional CO(2) Laser Resurfacing for Atrophic Post-Acne Scars: A Split-Face Clinical Trial," *Journal of Dermatological Treatment* 32, no. 2 (2021): 242–249, <https://doi.org/10.1080/09546634.2019.1630701>.